Thermal conductivity enhancement dependent pH and chemical surfactant for Cu-H$_2$O nanofluids

X.F. Li [a,*], D.S. Zhu [a], X.J. Wang [a,b], N. Wang [a], J.W. Gao [a], H. Li [a]

[a] *Key Lab of Enhanced Heat Transfer and Energy Conservation, Ministry of Education, School of Chemical and Energy Engineering, South China University of Technology, Guangzhou, Guangdong 510641, PR China*
[b] *Navy Arms of Services Command Academy, Guangzhou, Guangdong 510431, PR China*

Abstract

Nanofluids have been attractive for the last few years with the enormous potential to improve the efficiency of heat transfer fluids. This work focuses on the effect of pH and sodium dodecylbenzenesulfonate (SDBS) surfactant on the thermal conductivity of nanofluids. The thermal conductivity was measured by a Hot Disk Thermal Constants Anlyser. The results showed that the thermal conductivity enhancements of Cu-H$_2$O nanofluids are highly dependent on the weight fraction of nanoparticle, pH values and SDBS surfactant concentration of nano-suspensions. The Cu-H$_2$O nanofluids with an ounce of Cu have noticeably higher thermal conductivity than the base fluid without nanoparticles, For Cu nanoparticles at a weight fraction of 0.001 (0.1 wt%), thermal conductivity was enhanced by up to 10.7%, with an optimal pH value and SDBS concentration for the highest thermal conductivity. Therefore, the combined treatment with both the pH and chemical surfactant is recommended to improve the thermal conductivity for practical applications of nanofluid.
© 2008 Elsevier B.V. All rights reserved.

Keywords: Nanofluid; Copper nanoparticle; Thermal conductivity; Zeta potential

1. Introduction

Together with the greatly increasing thermal load in microelectronics and higher-powered automobiles, the needs for highperformance heating or cooling fluids are increasing every year. The thermal conductivity of these fluids plays a vital role in the development of energy-efficient heat transfer equipment. However, conventional heat transfer fluids have poor heat transfer properties compared to most solids. Since 1995 when U.S. Choi showed the possibility of using a new type of fluid containing nanoparticles [1], large enhancements of up to more than 100% in effective thermal conductivity (K_{eff}) of such fluids have been reported. The promising prospect for the fluid, *nanofluids*, triggered many researchers to find the best combination of particles and solvents [2–9] and to elucidate the governing mechanisms [10–15] as well. Keblinski et al. [14] suggested the

potential mechanisms for thermal conductivity enhancement such as Brownian motion, liquid layering and nanoparticle clustering. Koo and Kleinstreuer [16] found that the role of Brownian motion is much more important than the thermophoretic and osmo-phoretic motions. Vadasz [17] demonstrated that the transient heat conduction process in nanofluids may provide a valid explanation for the apparent heat transfer enhancement.

Because of the aforementioned complexity and contradiction in nanofluids, the research community has not reached a solid consensus on the mechanisms. Here, we take notice of the suspension stability as a common factor in the current technological limitations. As the surface chemical treatment changes the suspension stability through surface charge states and resultant surface potential [18,19].

Therefore, in the present study we change pH of the suspension systematically to control surface potential that can be reflected by zeta potential. The effects of the pH value of the aqueous suspension, sodium dodecylbenzenesulfonate (SDBS) concentration, and the weight fraction of the dispersed Cu particles on the enhanced thermal conductivity ratio have
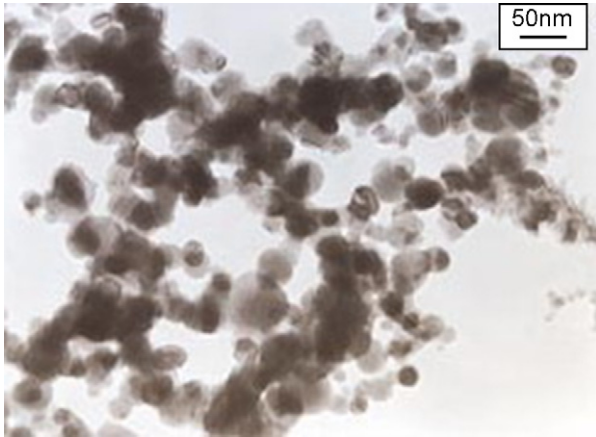
Fig. 1. TEM micrograph of nano-copper.

Fig. 3. Schematic diagram of TPS sensor.

Malvern ZS Nano S analyzer (Malvern Instrument Inc., London, UK). The measurement was run at $V = 10$ V, $T = 25\,°C$ with switch time at $t = 50$ s. Each experiment was repeated at least ten times to calculate the mean value of the experimental data. The pH value of system was adjusted with HCl and NaOH solution by precise pH Meter (PHS-25, China).

been investigated. It is expected to provide guidance to design nanofluids with excellent performance.

2. Experimental

2.1. Chemical

Cu powder (Shenzhen Junye Nano Material Ltd., China) with copper content >99.9% was used in the study. The transmission electron micrograph (TEM) of Cu powder is shown in Fig. 1. In Fig. 1, there are a few larger particles, which are likely aggregates of the smaller ones, but the whole distribution of the particles is relatively well-dispersed. The particles are basically spherical or near spherical. Particle size is relatively consistent with a unimodal distribution and an average diameter of 25 nm.

An anionic surfactant, sodium dodecylbenzenesulfonate (referred to as SDBS) in chemical grade, from Guangzhou Chemical Reagent Factory (China), was used. The surfactant structure is shown in Fig. 2. The water was purified by a Milli-Q Academic Millipore system. The pH was controlled using hydrochloric acid (HCl) and sodium hydroxide (NaOH) in analytical grade. All chemicals were used as received without any further purification.

2.2. Measurement of zeta potential and particle size

The experiments were conducted using 0.05 wt% copper nano-suspensions. Different concentrations of the surfactant were added to the suspensions, which were stirred thoroughly and ultrasonicated (KQ2200DE Ultrasonic Cleanser, 100 W, Kunshan of Jiangsu Equipment Company, China) for at least 15 min, 2–4 ml of suspensions was transferred into a measuring cell. Then zeta potential and particle size were measured by a
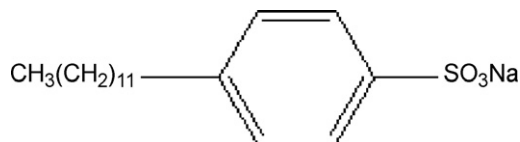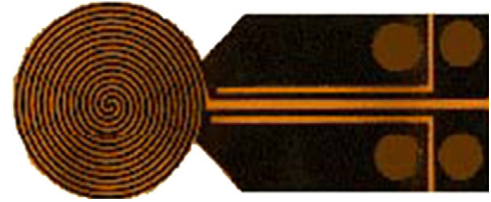

Fig. 2. Chemical structure of SDBS surfactant.

3. Measurement of the thermal conductivity of nanofluids

3.1. Transient plane source (TPS) theory

Thermal conductivity of nanofluids is measured by means of the TPS method [20]. In this method, the TPS element behaves both as temperature sensor and heat source. This novel method offers some advantages such as fast and easy experiments, wide range of thermal conductivities (from 0.02 to 200 W/m K), no sample preparation and flexible sample size.

The TPS element consists of an electrical conducting pattern of thin nickel foil (10 μm) in the form of double spiral, which resembles a hot disk, embedded in an insulating layer made of kapton (70 μm) (see Fig. 3).

A Kapton insulated probe is dipped into the suspensions. A constant electric power is supplied to the sensor and the increase in temperature $\Delta T(\tau)$ is calculated from the variation in the sensor resistance with time $R(t)$ by using the equation:

$$\Delta T(\tau) = \frac{1}{\alpha}\left(\frac{R(t)}{R_0} - 1\right) \tag{1}$$

where R_0 is the hot-disk resistance in the beginning of the recording (initial resistance), α is the temperature coefficient of resistance of the nickel foil, and $\Delta T(\tau)$ is the temperature increase of the sensor expressed in terms of an only variable τ, defined as:

$$\tau = \sqrt{\frac{t}{\theta}}, \; \theta = \frac{a^2}{\kappa} \tag{2}$$

where t is the measurement time, θ is the characteristic time, which depends both of parameters of the sensor (a is the sensor radius) and the sample (k is the thermal diffusivity of the sample).

Fig. 4 shows the sensor temperature variation in a typical transient heating.

Assuming the conductive pattern to be in the Y–Z plane of a coordinate system, the temperature rise at a point (y, z) at time t due to an output of power per unit area Q is given by the
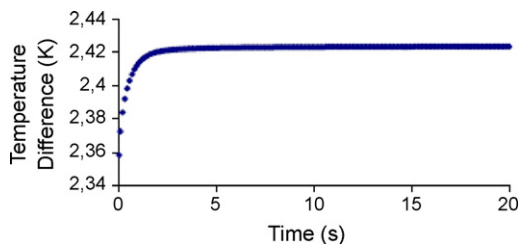
Fig. 4. Sensor temperature variation during a TPS measurement.

Table 1
Thermal conductivity of deionized water

T (K)	k_{exp} (W/m K)	k_{ref} (W/m K)	$k_{exp} - k_{ref}/k_{ref}$ (%)
283	0.5706	0.5741	−0.61
293	0.6010	0.5985	0.42
303	0.6233	0.6171	1.00

expression:

$$\Delta T(y, z, t) = (8\pi^{3/2}\rho c)^{-1} \int_0^\tau d\tau [k(t - t')]^{3/2} \int_A dy' dz'$$

$$\times Q(y', z', t')\exp\left\{-\left[\frac{(y - y')^2 + (z - z')^2}{4k(t - t')}\right]\right\} \tag{3}$$

where ρ is the density of the material (kg/m^3), c is the specific heat of the sample (J/Kg K) and k is the thermal diffusivity (m^2/s).

Previous expression can be simplified taking $k(t-t') = \sigma^2 a^2$:

$$\Delta T(y, z, t) = (4\pi^{3/2}a\lambda)^{-1} \int_0^\tau \frac{d\sigma}{\sigma^2} \int_A dy' dz' \times Q(y', z', t')$$

$$\times \exp\left\{-\left[\frac{(y - y')^2 + (z - z')^2}{4\sigma^2 a^2}\right]\right\} \tag{4}$$

where $k = \lambda/\rho c$ and λ is the thermal conductivity.

In the case of a disk geometry, consisting of m concentric ring sources, an exact solution of Eq. (4) is possible. The increase of temperature is:

$$\Delta T(\tau) = P_0(\pi^{3/2}a\lambda)^{-1} D(\tau) \tag{5}$$

where P_0 is the total output power and $D(\tau)$ is a geometric function given by the next expression:

$$D(\tau) = [m(m + 1)]^{-2} \times \int_0^\tau \frac{d\sigma}{\sigma^2} \left[\sum_{l=1}^{m} l \left\{\sum_{k=1}^{m} k\right.\right.$$

$$\left.\left.\times \exp\left(\frac{-(l^2 + k^2)}{4\sigma^2 m^2}\right) I_0\left(\frac{lk}{2\sigma^2 m^2}\right)\right\}\right] \tag{6}$$

in which I_0 is the modified Bessel function.

By fitting the experimental data to the straight line given by Eq. (5), the thermal conductivity can be obtained by calculating the value of slope for the fitting line ($P_0/(\pi^{3/2}a\lambda)$).

3.2. Measurement process of the thermal conductivity of nanofluids

Different concentration nano-suspensions were prepared, which were stirred thoroughly and ultrasonicated for half of an hour. A Kapton insulated probe (design 7577) was successively dipped into the different nano-suspensions. The diameter of the sensing spiral in the probe was about 2.001 mm and the

Kapton insulation on both sides of the spiral had a thickness of 13 μm. Then the thermal conductivity was measured by a Hot Disk Thermal Constants Anlyser (Hot Disk Inc., Uppsala, Sweden). The measurement was run at $V = 0.02$ V, $T = 25$ °C with switch time at $t = 5$ s. Each experiment was repeated at least ten times to calculate the mean value of the experimental data. The pH value of system was adjusted with HCl and NaOH solution by precise pH Meter (PHS-25, China).

Before systematic experiments were performed on Cu-H$_2$O nanofluids, the experimental system was tested with deionized water as the working fluid. The results with the deionized water will also serve as the basis for comparison with the results of nanofluids (see Table 1). The uncertainty of our measurements is calculated to be less than ±1.00%.

4. Results and discussion

4.1. Preparation of nanofluids

Ultrasonication was used for preparation of mixed aqueous nano-suspensions, which is an accepted technique for dispersing the highly entangled or aggregated nanoparticle samples [21,22], but longer time of high-energy sonication can introduce defects. In the study, copper nanoparticle (0.1 g) and a water solution (99.8 g) with SDBS surfactant (0.1 g) were directly mixed in a 150-ml beaker. The suspension was transferred into an ultrasonic vibrator and sonicated for 1 h at a frequency of 40 kHz and an output power of 100 W at 25–30 °C. For the comparison, the suspension without SDBS surfactant was sonicated for 1 h in the same way. Fig. 5 illustrates the particle size distributions of Cu-H$_2$O nano-suspensions in the absence (a) and in the pres-
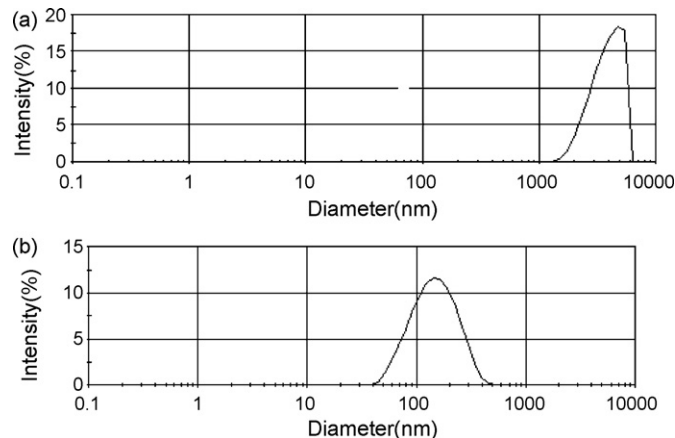

Fig. 5. Particle size distributions of Cu-H$_2$O suspensions in the absence (a) and in the presence (b) of SDBS surfactant. Concentration of Cu and SDBS surfactant are 0.05 wt%.
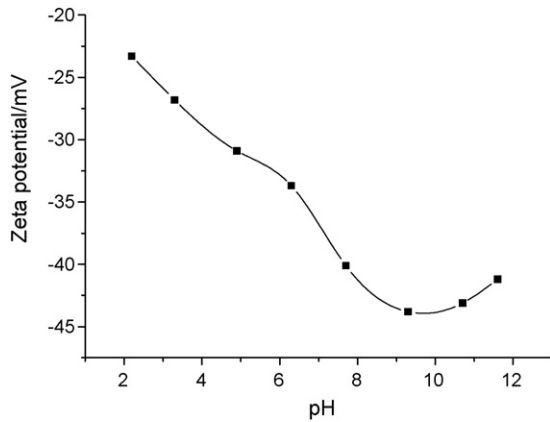
Fig. 6. Effect of pH on zeta potential of Cu-H$_2$O suspensions with SDBS surfactant. Concentration of Cu and surfactant are 0.05 wt%.

Fig. 8. Effect of SDBS concentration on thermal conductivity of Cu-H$_2$O suspensions.

ence (b) of SDBS surfactant, which shows that there are obvious variations in the particle size characteristics between two samples. The average particle sizes obtained are (a) in the absence of SDBS surfactant: 6770 nm, (b) in the presence of SDBS surfactant: 207 nm. Therefore, the stabilization of Cu-H$_2$O suspension with SDBS surfactant is better.

4.2. Influence of pH on thermal conductivity of copper nano-suspensions

Fig. 6 shows the change of zeta potential for Cu-H$_2$O suspensions with SDBS surfactant as a function of pH. According to the zeta potential values of copper powders, pH 8.5–9.5 can be selected as an operating pH for the suspensions with SDBS surfactant. Because, in the pH, the absolute values of zeta potential for Cu-H$_2$O suspensions with SDBS surfactant is higher, so there are more surface charges around the particles.

Fig. 7 shows the change of thermal conductivity ratio for Cu-H$_2$O suspensions with SDBS surfactant as a function of pH. It can be seen that the thermal conductivity ratio increases as pH increases from 3 to 8.5–9.5. As addressed in the literatures [9,23], such abnormal enhancements are not explained by any pre-existing model. When the nanoparticles are dispersed into water, the overall behavior of the particle–water interac-
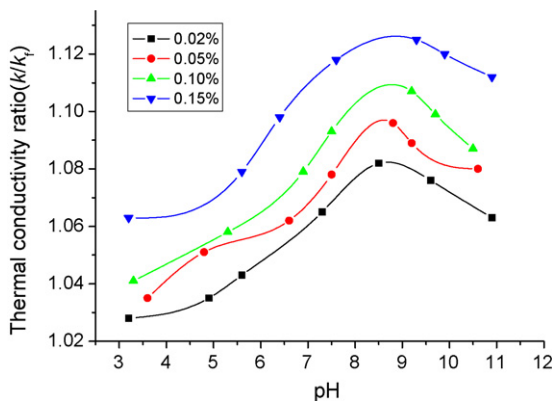
tion depends on the properties of the particle surface. At the isoelectric point (IEP), the repulsive forces among copper particles is zero and nanoparticles will coagulate together under this pH value. Therefore, when the pH value is equal to or close to the IEP, copper particle suspension is unstable according to the DLVO theory [24–26]. The hydration forces among particles increase with the increasing difference of the pH value of a suspension from the IEP, which results in the enhanced mobility of nanoparticles in the suspension. The microscopic motions of the particles cause microconvection that enhances the heat transport process. So we attempt to link the concept of surface charges to the change in thermal conductivity ratio of nanofluids. The point to mention is that the charged surface sites seemingly provide much more effective passages through which heats or phonons are going more efficiently. Lee et al. [18] showed that surface charge states are mainly responsible for the increase of thermal conductivity in the present condition by a surface complexatio model for the measurement data of hydrodynamic size, zeta potential, and thermal conductivity. Xue et al. [27] showed from molecular dynamic simulation that phonons felt much less resistance during travel from particle to liquid at stronger interfacial bonding. Therefore, it looks reasonable to infer that optimizing pH or higher surface charging condition facilitates phonon transport through increases of effective sites and transport efficiency.

As depicted in Fig. 6, as the pH goes away from the IEP, the surface charge increases because of more frequent attacks to the surface hydroxyl groups and phenyl sulfonic group by potential-determining ions (H$^+$, OH$^-$ and phenyl sulfonic group), leading to an increase in the zeta potential on the copper powder surface. In this way, we can infer that there are more surface charges at pH 8.5–9.5, at which the dispersion behavior is better and the thermal conductivity is higher. As expected, the surface charge is minimum at the IEP.

4.3. Influence of the surfactant concentration on thermal conductivity of copper nano-suspensions

Fig. 8 presents the thermal conductivity ratio of the Cu-H$_2$O suspensions and the base fluid with respect to the concentration of SDBS surfactant at pH 8.5–9.5. The weight fraction of the

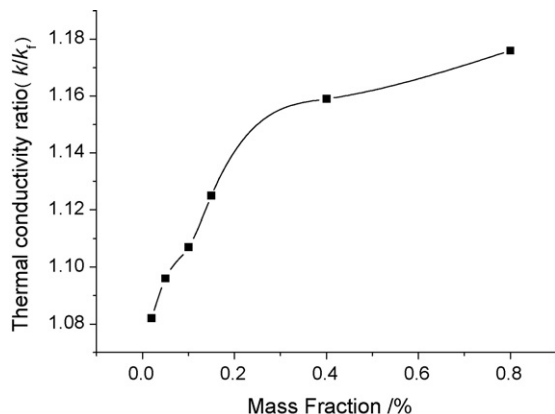Fig. 7. Effect of pH on thermal conductivity of Cu-H$_2$O suspensions with SDBS surfactant.

Fig. 9. Thermal conductivity ratio of Cu-H$_2$O suspensions as a function of solid weight fraction.

Cu-H$_2$O suspensions is 0.1 wt%. For the base fluid, the thermal conductivity ratio starts to decrease after a certain value of the surfactant concentration. In the present experiments, the highest thermal conductivity appears at 0.02 wt% water solution, which means when an ounce of SDBS surfactant is added, the thermal conductivity at 0.02 wt% water solution is higher than that of pure water. In the 0.1 wt% Cu-H$_2$O suspensions, the trend of the variation of the thermal conductivity is very similar to those in the base fluid with surfactant only. However, the thermal conductivity ratio decreases slowly as SDBS concentration increases from 0.02 wt% to 0.10 wt%, and then decreases very quickly with an increase in the SDBS concentration. Obviously, For the Cu-H$_2$O suspensions and the base fluid, when more SDBS is added into the systems, the thermal conductivity ratios decrease very quickly. Owing to this trend, the addition of more surfactant seems noneffective in the Cu-H$_2$O suspensions. This is because the heat transfer area becomes narrower due to the amount of the surfactants on the particle surface. Taking into account the combined effect of dispersion behavior and thermal conductivity, the 0.10 wt% SDBS can be selected as an optimizing concentration for the 0.1% copper nano-suspensions. Therefore, it can be concluded that the application of nanofluid with optimizing chemical surfactant is a better way among the considered enhancement techniques in the viewpoint of the effectiveness of dispersion behavior and thermal conductivity.

4.4. Influence of the weight fraction of nanoparticle on thermal conductivity of copper nano-suspensions

Fig. 9 shows the enhanced thermal conductivity ratio of Cu-H$_2$O suspensions with the optimizing SDBS concentration as a function of the weight fraction of nanoparticle. pH 8.5–9.5 can be selected as an operating pH for different weight fraction suspensions. The results show that an ounce of nanoparticle suspensions have noticeably higher thermal conductivities than the base fluid without nanoparticles. The thermal conductivity of Cu-H$_2$O nanofluid is enhanced approximately nonlinearly with the weight fraction of the copper nanoparticle, it implies that Cu-H$_2$O suspensions can enhance the

heat transfer performance. The maximum thermal conductivity enhancements of up to 10.7% is observed at the 0.10 wt% suspension.

5. Conclusions

This paper is concerned with the thermal conductivity of Cu-H$_2$O nanofluid under different pH values and different sodium dodecylbenzenesulfonate (SDBS) concentration, and the thermal conductivity of nanofluids are measured by the transient plane source method. Key conclusions can be summarized as follows:

1. Cu-H$_2$O nanofluids by two-step method were prepared. The particle size distribution show better dispersion behavior in the suspension with the addition of surfactant.
2. We have shown that the pH of the nanofluid strongly affects the thermal conductivity of the suspension. As the pH of the nanofluid goes far from the IEP, the surface charge increases because of more frequent attacks to the surface hydroxyl groups and phenyl sulfonic group by potential-determining ions (H$^+$, OH$^-$ and phenyl sulfonic group), and the colloidal particles get more stable and eventually alter the thermal conductivity of the fluid. In this way, we can infer that there are more surface charges at pH 8.5–9.5, at which the thermal conductivity is higher.
3. The use of Cu nanoparticles as the dispersed phase in water can significantly enhance the thermal conductivity, and the enhancement increases with particle concentration under the conditions of this work. The maximum thermal conductivity enhancements of up to 10.7% is observed at the 0.10 wt% suspension.
4. The thermal conductivity can be improved by adding optimizing SDBS surfactant. However, the combined treatment with both the pH and chemical surfactant is recommended to improve the thermal conductivity for practical applications of nanofluid.

Acknowledgements

References

[1] S.U.S. Choi, ASME 231 (1995) 99.
[2] K. Hong, T.-K. Hong, H.-S. Yang, Appl. Phys. Lett. 88 (3) (2006) 31901.
[3] C.H. Li, G.P. Peterson, J. Appl. Phys. 99 (8) (2006) 084314.
[4] S.K. Das, N. Putra, P. Thiesen, W. Roetzel, J. Heat Transf. 125 (2003) 567.
[5] X.F. Li, D.S. Zhu, X.J. Wang, J. Colloid Interface Sci. 310 (2007) 456.
[6] J.A. Eastman, S.U.S. Choi, S. Li, L.J. Thompson, Mater. Res. Soc. 457 (1997) 3.
[7] Y. Hwang, J.K. Lee, C.H. Lee, et al., Thermochim. Acta 455 (2007) 70.

[8] X.F. Li, D.S. Zhu, Chem. Ind. Eng. Progress 25 (2006) 875.

[9] H.E. Patel, S.K. Das, T. Sundararagan, A.S. Nair, B. Geoge, T. Pradeep, Appl. Phys. Lett. 83 (2003) 2931.

[10] D.H. Kumar, H.E. Patel, V.R.R. Kumar, T. Sundararajan, T. Pradeep, S.K. Das, Phys. Rev. Lett. 93 (2004) 144301.

[11] S.P. Jang, S.U.S. Choi, Appl. Phys. Lett. 84 (2004) 4316.

[12] Q. Xue, W.M. Xu, Mater. Chem. Phys. 90 (2005) 298.

[13] Y.M. Xuan, Q. Li, W. Hu, AIChE J. 49 (2003) 1038.

[14] P. Keblinski, S.R. Phillpot, S.U.S. Choi, J.A. Eastman, Int. J. Heat Mass Transf. 45 (2002) 855.

[15] B.X. Wang, L.P. Zhou, X.F. Peng, Int. J. Heat Mass Transf. 46 (2003) 2665.

[16] J. Koo, C. Kleinstreuer, Int. Commun. Heat Mass Transf. 32 (9) (2005) 1111.

[17] P. Vadasz, J. Heat Transf. 128 (5) (2006) 465.

[18] D. Lee, J.-W. Kim, B.G. Kim, J. Phys. Chem. B 110 (9) (2006) 4323.

[19] R.J. Hunter, Foundations of Colloid Science, first ed., Clarendon Press, Oxford, 1987.

[20] M.A. Rodríguez-Pérez, J.A. Reglero, D. Lehmhus, M. Wichmann, J.A. de Saja, A. Fernández, International Conference "Advanced Metallic Materials", Smolenice Slovakia November, 2003, p. 253.

[21] X.F. Li, D.S. Zhu, X.J. Wang, J.W. Gao, H. Li, Proceedings of the International Symposium on Biophotonics, Nanophotonics and Metamaterials, Hangzhou, China October, 2006, p. 363.

[22] M. Lindheimer, E. Keh, S. Zaini, S. Partyka, J. Colloid Interface Sci. 138 (1990) 83.

[23] H. Xie, H. Lee, W. Youn, M. Choi, J. Appl. Phys. 94 (2003) 4967.

[24] W.B. Russel, D.A. Saville, W.R. Schowwalter, Colloidal Suspensions, Cambridge University Press, Cambridge, 1989.

[25] R.J. Hunter, Foundations of Colloid Science, vol. 1, Clarendon Press, Oxford, 1987.

[26] M. Elimelech, J. Gregory, X. Jia, R.A. Williams, Particle Deposition and Aggregation: Measurement, Modeling and Simulation, Butterworths, Oxford, 1995.

[27] L. Xue, P. Keblinski, S.R. Phillpot, S.U.S. Choi, J.A. Eastman, J. Chem. Phys. 118 (2003) 337–339.